# Influence of ambient groundwater flow on DNAPL migration in a fracture network: Experiments and simulations

Sung-Hoon Ji, In Wook Yeo, and Kang-Kun Lee
School of Earth and Environmental Sciences, Seoul National University, Seoul, South Korea

Robert J. Glass
Flow Visualization and Processes Laboratory, Sandia National Laboratories, Albuquerque, New Mexico, USA

Received 5 February 2003; revised 4 March 2003; accepted 15 April 2003; published 20 May 2003.

[1] We consider the influence of ambient groundwater flow on the migration of DNAPL within a fracture network. In context of a modified invasion percolation (MIP) growth algorithm, we formulate a mechanistic model that includes capillary and gravity forces as well as viscous forces within the DNAPL and the ambient groundwater. The MIP model is verified against laboratory experiments, which show good agreement in DNAPL migration path through a two-dimensional fracture network. The results of both simulations and laboratory experiments suggest that ambient groundwater flow can be a significant factor controlling DNAPL migration path, velocity, and channeling pattern in a fracture network. *INDEX TERMS:* 5104 Physical Properties of Rocks: Fracture and flow; 5139 Physical Properties of Rocks: Transport properties; 5114 Physical Properties of Rocks: Permeability and porosity. **Citation:** Ji, S.-H., I. W. Yeo, K.-K. Lee, and R. J. Glass, Influence of ambient groundwater flow on DNAPL migration in a fracture network: Experiments and simulations, *Geophys. Res. Lett.*, *30*(10), 1504, doi:10.1029/2003GL017064, 2003.

## 1. Introduction

[2] Groundwater contamination by dense nonaqueous phase liquids (DNAPLs), such as trichloroethylene (TCE), is one of the most pressing problems in contaminant hydrology today. Because DNAPL is denser than water, it migrates downward through the overlying sediments and often reaches the underlying bedrock. There, it enters ever-present fractures that dissect the bedrock and forms a long-term source of contamination due to its low solubility in water.

[3] While the study of DNAPL contamination in sediments has received significant attention, far less research has considered the underlying fractured rock. The problem is one of first, understanding DNAPL migration within fractured rock and second, understanding its subsequent dissolution and thus contaminant loading of the groundwater system. Within the topology of the fracture network where individual rough walled fractures intersect, migration of the liquid phase DNAPL is governed by the interplay of capillary, gravity, and viscous forces [e.g., *Kueper and McWhorter*, 1991]. Dissolution can take place into the water flowing in individual fractures [e.g., *Detwiler et al.*, 2001] or into the surrounding matrix if porous [e.g., *Parker et al.*, 1994, 1997; *VanderKwaak and Sudicky*, 1996].

[4] To understand the processes that govern DNAPL migration, mechanistic models formulated below the usual scale of porous-continuum averaging, are of great use. Such models often begin with modifications of invasion percolation (IP). In IP, the phase invasion process is simulated through application of a simple growth algorithm that includes local capillary forces. Since its introduction by *Wilkinson and Willemsen* [1983], IP has been modified (MIP) in many ways such as to include gravity/buoyancy forces [*Meakin et al.*, 1992], as well as viscous forces [*Xu et al.*, 1998]. In context of DNAPL migration, *Glass et al.* [2001] developed a macro-modified invasion percolation (MMIP) model, incorporating the influences of capillary, gravity, and viscous forces within the invading phase to simulate experiments conducted in macro-heterogeneous porous media.

[5] Over the past few years, MIP has also been applied to immiscible displacements in single fractures [see review *Glass et al.*, 2001]. In this context, MIP has been further augmented to include in-plane curvature at the phase interface [*Glass et al.*, 1998], the simultaneous invasion of two fluids to capture the phase fragmentation process in horizontal [*Amundsen et al.*, 1999] and vertical [*Glass and Yarrington*, 2003] fractures, as well as applied to correlated aperture fields [*Wagner et al.*, 1999; *Steele and Lerner*, 2001].

[6] In this paper, we apply MIP to DNAPL migration within fracture networks. In particular, we are interested in the influence of the ambient groundwater flow within the fracture network on DNAPL migration. We first modify MIP to include this influence through the hydraulic gradient within the groundwater. To test our model, we then design a transparent fracture network and conduct two experiments that vary the influence of ambient groundwater flow. The results of both our model and experiments show that ambient groundwater flow can significantly influence the migration of DNAPL within fracture networks.

## 2. Conceptualization of MIP Model

[7] To model the influence of ambient groundwater flow on DNAPL migration within a fracture network, we develop and apply a mechanistic growth algorithm that is a modification of IP. In IP, random numbers (''invadability'')are assigned to each site on a lattice representing a random medium. Initially, all sites are occupied by the ''defender fluid'' and then one site is occupied by the ''invader fluid''


0094-8276/03/2003GL017064$05.00

at its point of injection. The IP algorithm works by repeating the following two steps: 1) Identify the defender fluid site adjacent to the invaded region; and 2) Invade the identified site that has the highest invadability.

[8] We modify IP to identify the invadability at each site with an invasion pressure due to local capillary, gravity, and viscous forces. Neglecting curvature in the plane of the fracture, the capillary pressure $P_c$ is given by the LaPlace-Young equation as:

$$P_c = -\frac{2\sigma\cos\theta}{e}, \tag{1}$$

where, $\sigma$ is the interfacial tension, $\theta$ is the contact angle with respect to the fracture plane (0 degrees for wetting and 180 degrees for nonwetting fluid invasion), and $e$ is the fracture aperture. The gravity pressure $P_g$ is represented by the density difference between wetting fluid and nonwetting fluid as:

$$P_g = \left(\rho_{invader} - \rho_{defender}\right) gz\sin\alpha, \tag{2}$$

where $\rho_{invader}$ and $\rho_{defender}$ are densities of invader and defender fluid, $g$ is the acceleration due to gravity, $z$ is the vertical thickness of invader fluid, and $\alpha$ is the dip angle of a fracture. The viscous pressure within the invader fluid $P_{vi}$ increases back to the point of injection as:

$$P_{vi} = \frac{Q_{invader}\mu_{invader}L}{kA}, \tag{3}$$

where $Q_{invader}$ is the local flow rate, $\mu_{invader}$ is the viscosity of the invader fluid, $L$ is the distance back along the flow path from the interface between the two fluids to the injection point, $k$ is the permeability of the fracture, and $A$ is the local cross-sectional area of the flow path. The viscous pressure within defender fluid $P_{vd}$ is given as:

$$P_{vd} = \rho_{defender} g h_{defender}, \tag{4}$$

where $h_{defender}$ is the viscous component of the local hydraulic head within the defender fluid due to ambient groundwater flow.

[9] Combining equations (1), (2), (3), and (4), the invadability for a site is defined as

$$I = \frac{2\sigma\cos\theta}{e} + (\rho_{invader} - \rho_{defender}) gz\sin\alpha + \frac{Q_{invader}\mu_{invader}L}{kA} - \rho_{defender} g h_{defender}. \tag{5}$$

For nonwetting fluid such as DNAPL, the capillary term in (5) is negative and thus invadability increases with aperture $e$. Likewise, the gravity term increases invadability for locations lower in the network as invasion proceeds. Finally, the viscous terms cause invadability to increase both back toward the point of injection, as well as downstream within the ambient groundwater flow field.

## 3. Experiments

[10] To test our MIP model, we designed a transparent experimental system that allowed visualization of the migration process (Figure 1). Cuts within a 20 cm tall × 15 cm wide x 2 cm thick acrylic plate created a two-dimensional fracture network using a laser-milling machine (FA-1200

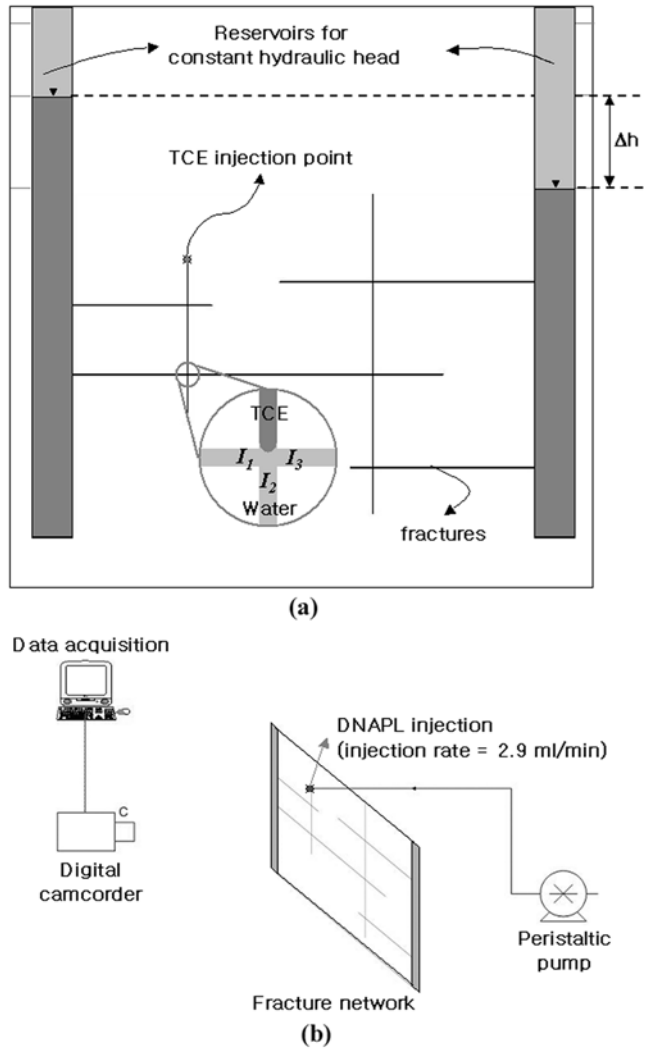


**Figure 1.** (a) A fracture network model used for experiments. Fractures have a constant aperture of 0.2 mm. (b) Schematic diagram of laboratory experiment setup.

Laser, Fawoo Inc.). Reservoirs on either end of the network allowed the variation of the ambient hydraulic gradient and thus groundwater flow. DNAPL was injected into one of the vertical fractures at a rate of 2.9 ml/min using a peristaltic pump. Fractures were of uniform aperture (0.2 mm) and constant width (2 cm), and were made hydrophilic by coating with $TiO_2$ followed by exposure to ultraviolet rays [*Watanabe et al.*, 1999]. Water ($\rho$ = 0.998 g/ml, $\mu$ = 1.000 cP at 25°C) and TCE ($\rho$ = 1.464 g/ml, $\mu$ = 0.576 cP at 25°C) formed the groundwater and DNAPL, respectively. The interfacial tension between the two fluids ($\sigma$ = 0.0238 ± 0.0003 N/m) was measured by a Processor Tensiometer K12 (KRÜSS Gmbh, Hamberg). For visualization, sulforhodamine B was added to water at concentration of 0.1 g/l. TCE migration was recorded with digital camcorders.

[11] The influence of ambient groundwater flow was demonstrated with two experiments: (i) case 1 - static hydraulic condition; (ii) case 2 – dynamic hydraulic condition with a $\Delta$h of 4 cm between the two reservoirs. While flow rates in case 2 were at the high end of what might be expected under natural conditions, calculations of flow

through the network yielded estimates of Reynolds numbers (*Re*) for flowing fractures that ranged from 0.60 to 1.55, well within the linear flow regime [*Zimmerman and Bodvarsson*, 1996].

[12] Figures 2a–2d show the TCE migration pattern for case 1 at several stages. Injected TCE migrated through the vertical fracture initially in a narrow channel ~ 20% of the fracture width (i.e., a gravity-driven finger) and filled up the dead-end fracture below the second intersection (Figure 2a). TCE then invaded both the right and left horizontal fractures at similar invasion rates in wide channels ~ 90% of the fracture width (Figure 2b). When TCE met the next vertical fracture to the right, it flowed downward and once again filled up the dead end region below (Figure 2c). Meanwhile, invading TCE to the left entered the left reservoir. Finally, the right reservoir was invaded through the lower horizontal fracture ~47 seconds from the start of injection (Figure 2d).

[13] For case 2, TCE migration began as in case 1 (Figures 3a–3d). However, after TCE filled the first dead-end fracture below the second intersection (Figure 3a), it migrated only to the right, downgradient within the ambient groundwater flow field (Figure 3b). Due to viscous forces within the flowing water, the channels of TCE in the horizontal fractures were only ~ 25% of the fracture width, much narrower than those of case 1, (Figures 3b and 3d), and TCE reached the right reservoir after only ~ 28 second from the start of injection.

## 4. Comparison of MIP to Experiment

[14] To implement MIP, the fracture network was discretized into a two-dimensional network within which the invadability, *I*,was calculated at each grid block or site. All fractures were considered to have the same properties

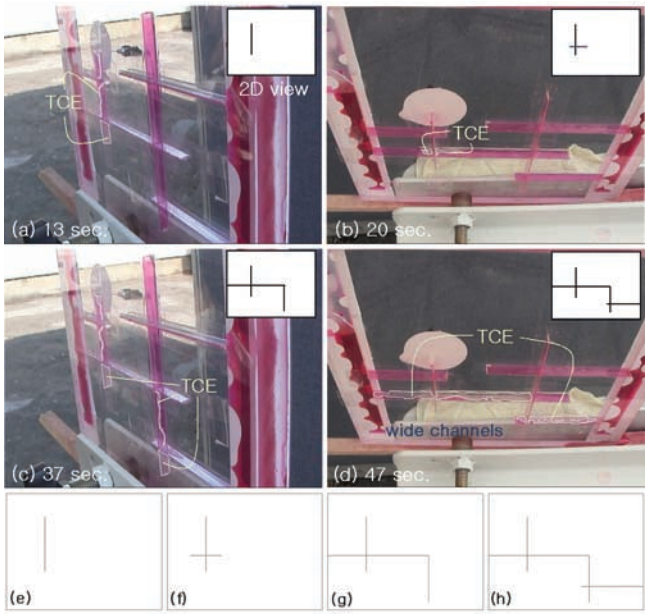


**Figure 2.** (a–d) TCE migration path observed during an experiment for case 1. TCE (colorless fluid) invades water (red fluid) with gravity-driven fingering in vertical fractures and wide flow channels within horizontal fractures. (e–h) Simulated TCE migration path by the MIP model.

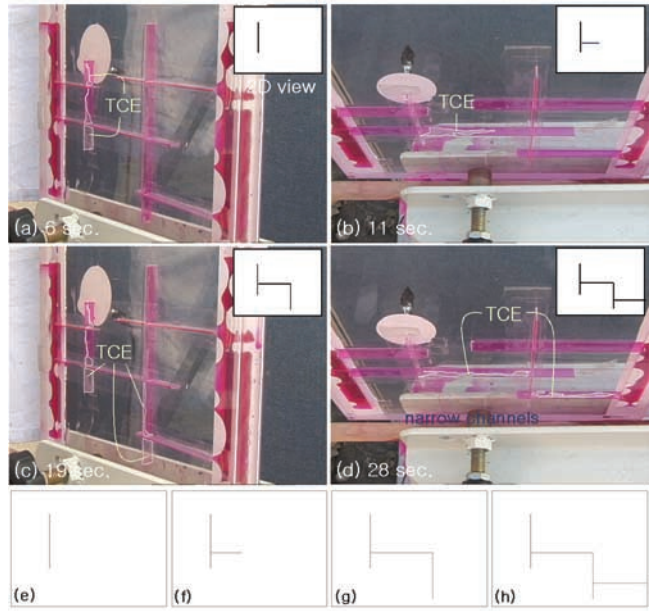


**Figure 3.** (a–d) TCE migration path observed during an experiment for case 2. TCE (colorless fluid) invades water (red fluid) with gravity-driven fingering in vertical fractures and narrow flow channels within horizontal fractures. (e–h) Simulated TCE migration path by the MIP model.

(*e, k, A*), fluid properties (ρ, μ, σ) were given by their measured values. $Q_{invader}$ was taken to be constant and equal to the imposed injection rate. TCE was assumed to be perfectly nonwetting such that cos θ = −1.

[15] Figures 2e–2h show the simulated migration path for case 1 and agreed well with experimental results. Injected TCE migrated downward within the vertical injection fracture until TCE reached the bottom of the dead-end fracture. From calculated invadabilities, this flow pattern was due entirely to gravity. TCE then moved into both the right and left horizontal fractures equally, as determined by the viscous forces within the TCE. These flow patterns were repeated until TCE invaded the right reservoir.

[16] For case 2, we obtain the pressure within the defending ambient groundwater flow field by using a finite element method to solve the steady state, single-phase viscous flow equation:

$$\frac{\partial}{\partial l}\left[\frac{k\rho_{defender}ge}{\mu_{defender}}\frac{\partial h}{\partial l}\right] = 0, \tag{6}$$

where $k$ is given by the cubic law. At each invasion step, the permeability of invaded site was adjusted for TCE-invaded area as observed from the experiment and equation (6) was re-solved to update the invadability for each site across the network. For case 2, after it invaded the vertical dead-end fracture below the second intersection (as in case 1), it flowed only into the right horizontal fracture (Figures 3e–3h). The choice of right over left at this intersection was due to the viscous influence within the ambient groundwater flow field. For case 1, the invadability to either the right or left (see intersection diagram in Figure 1a) is indistinguishable. However, for case 2, $I_1$ to the left is lower than $I_3$ to the right because it

is upgradient within the groundwater flow field and thus TCE invades only the fracture to the right.

## 5. Summary and Conclusions

[17] Both MIP simulations and experimental results suggest that ambient groundwater flow can significantly influence the migration of DNAPL in fracture networks. Additionally, experiments indicate that migration velocity as well as the sub-scale phase structure within fractures will be influenced. While these additional effects are not yet represented within the current MIP model, it is able to well capture the migration pathway through the network. Further model development to include individual fractures as two-dimensional objects with variable aperture will allow gravity-driven fingering, viscous fingering, and aperture induced channeling to develop naturally as invasion progresses. Thus, our study provides a stepping-stone in the development of reliable numerical simulators for DNAPL migration in fracture networks that can increase our understanding of process. Such understanding is required to implement rational and cost-effective risk assessment procedures for DNAPL-contaminated fractured bedrock.

[18] **Acknowledgments.** This study was financially supported by the BK 21 project of the Korean Government and a grant (code : 3-5-1) from Sustainable Water Resources Research Center of 21st Century Frontier Research Program. We thank Electronic Functional Materials Laboratory of Seoul National University and Self-assembling Molecules & Nanoparticles Laboratory of Hanyang University for their helps in $TiO_2$ coating and interfacial tension measurement. RJG acknowledges support from the U.S. Department of Energy's Environmental Management Science Program under contract DE-AC04-94AL85000. We are grateful to two anonymous reviewers for their constructive comments.

## References

Amundsen, H., G. Wagner, U. Oxaal, P. Meakin, J. Feder, and T. Jøssang, Slow two-phase flow in artificial fractures: experiments and simulations, *Water Resour. Res.*, *35*(9), 2619–2626, 1999.

Detwiler, R., H. Rajaram, and R. J. Glass, Nonaqueous-phase liquid dissolution in variable-aperture fractures: Development of a depth-averaged computational model and comparison to a physical experiment, *Water Resour. Res.*, *37*(12), 3115–3129, 2001.

Glass, R. J., M. J. Nicholl, and L. Yarrington, A modified invasion percolation model for low-capillary number immiscible displacements in horizontal rough-walled fractures: Influence of local in-plane curvature, *Water Resour. Res.*, *34*(12), 3215–3234, 1998.

Glass, R. J., H. Rajaram, M. J. Nicholl, and R. L. Detwiler, The interaction of two fluid phases in fractured media, *Current Opinion in Colloid & Interface Science*, *6*, 223–235, 2001.

Glass, R., J. Conrad, and S. H. Yarrington, Gravity-destabilized nonwetting phase invasion in macroheterogeneous porous media: near-pore-scale macro modified invasion percolation simulation of experiments, *Water Resour. Res.*, *37*(5), 1197–1207, 2001.

Glass, R. J., and L. Yarrington, Mechanistic modeling of fingering, nonmonotonicity, fragmentation, and pulsation within gravity/buoyant destabilized two–phase/unsaturated flow, *Water Resour. Res.*, *39*(3), 1058, doi:10.1029/2002WR001542, 2003.

Kueper, B. H., and D. B. McWhorter, The behavior of dense, nonaqueous phase liquids in fractured rock and clay, *Ground Water*, *29*(5), 716–728, 1991.

Meakin, P., J. Feder, V. Frette, and T. Jøssang, Invasion percolation in a destabilizing gradient, *Phys. Rev. A.*, *46*(6), 3357–3368, 1992.

Parker, B. L., R. W. Gillham, and J. A. Cherry, Diffusive disappearance of immiscible-phase organic liquids in fractured geologic media, *Ground Water*, *32*(5), 805–820, 1994.

Parker, B. L., D. B. McWhorter, and J. A. Cherry, Diffusive loss of nonaqueous phase organic solvents from idealized fracture networks in geologic media, *Ground Water*, *35*(6), 1077–1088, 1997.

Steele, A., and D. N. Learner, Predictive modeling of NAPL injection tests in variable aperture spatially correlated fractures, *J. of Cont. Hydrol.*, *49*(3–4), 287–310, 2001.

VanderKwaak, J. E., and E. A. Sudicky, Dissolution of non-aqueous liquids and aqueous-phase contaminant transport in discretely-fractured porous media, *J. of Cont. Hydrol.*, *23*(1–2), 45–68, 1996.

Wagner, G., P. Meakin, J. Feder, and T. Jøssang, Invasion percolation in fractal fractures, *Physica A*, *264*, 321–337, 1999.

Watanabe, T., A. Nakajima, R. Wang, M. Minabe, S. Koizumi, A. Fujishima, and K. Hasimoto, Photocatalytic activity and photoinduced hydrophilicity of titanium dioxide coated glass, *Thin Solid Films*, *351*, 260–263, 1999.

Wilkinson, D., and J. F. Willemsen, Invasion percolation: A new form of percolation theory, *J. Phys. A Math. Gen.*, *16*, 3365–3376, 1983.

Xu, B., Y. C. Yortsos, and D. Salin, Invasion percolation with viscous forces, *Phys. Rev. E*, *57*(1), 739–751, 1998.

Zimmerman, R. W., and G. S. Bodvarsson, Hydraulic conductivity of rock fractures, *Transport in Porous Media*, *23*, 1–30, 1996.

S.-H. Ji, I. W. Yeo, and K.-K. Lee, School of Earth and Environmental Sciences, Seoul National University, Seoul 151–747, Korea. (ji0511@snu.ac.kr; iwyeo@snu.ac.kr; kklee@snu.ac.kr)

R. J. Glass, Flow Visualization and Processes Laboratory, Sandia National Laboratories, Albuquerque, NM USA. (rjglass@sandia.gov)